STRUCTURE FUNCTIONS AND THEIR IMPLICATIONS FOR HIGHER RESOLUTION ANALYSIS

Peter Lönnberg

European Centre for Medium Range Weather Forecasts

Reading, U.K.

1. INTRODUCTION

The purpose of an assimilation scheme is to produce accurately the initial state of all modes which are important for forecasting. In an ideal situation with perfect observations and uniform data distribution this goal could be easily achieved. However, imperfect and irregularly distributed observations, together with computational limitations, impose on an analysis scheme constraints that narrow its spectral width. This study is confined to the problems of horizontal resolution - the vertical problem has been treated by Andersen (1983).

Local analysis schemes, like statistical interpolation (OI), view the atmosphere through a narrow spectral window. For synoptic scale disturbances local schemes generally respond well. Naturally, the analysis response drops as the size of the disturbance approaches the data density. The large scale analysis is a combination of several local estimates of the atmospheric state and a deterioration is inevitable for low wavenumbers (Cats and Wergen, 1983). This paper will concentrate on the problems of analysing small scale features, such as developing baroclinic waves, polar lows etc.

In Section 2 the analysis response is quantified as a function of scale and observation error for a univariate two-dimensional OI scheme, which has a structure which resembles the ECMWF (EC) system. Important factors such as data density, the size of the analysis volume and the specified observation errors are discussed. The impact on analysis resolution of varying the assumed characteristic scale parameter of the forecast error model is studied

by idealised experiments and analyses of an intense small scale cyclone using real data.

The strong damping effect of the exponential correlation function (that is the Gaussian function) at high wavenumbers has been demonstrated by Julian and Thiebaux (1975). An alternative representation of the horizontal forecast error correlation, by a series of Bessel functions, is compared to the Gaussian correlation function as regards its fit to the observed error structures and its impact on resolution in a univariate scheme (Section 3). The real data case of Section 2 is repeated using the Bessel function correlation model.

The expansion of the OI operator in terms of eigenvectors and eigenvalues provides a different method of studying the resolution (Section 4). We find that the sensitivity to the specified horizontal correlation model is clearly demonstrated.

Section 5 summarizes the possibilities of improving the resolution of the EC analysis scheme.

2. AMPLITUDE RESPONSE OF OI

The specification of reasonable statistics for forecast and observation errors is of central importance in statistical interpolation. Ideally, the error covariance structures should depend on the situation they are applied to and should be defined by the data used in the calculations or by the flow type. In practice, however, the correlation models are fixed and only the magnitudes of the errors vary in time. If the chosen correlation models are representative of long-term error statistics, we can expect good analyses in most situations. Unfortunately, situations of meteorological significance tend to have error properties that differ from the mean situation. The implications on the analysis of using non-optimal statistics will now be discussed.

2.1 Analysis of height

An attempt to determine the horizontal analysis resolution is made by simulating the EC system two-dimensionally and univariately (for details of the EC analysis scheme see Lorenc, 1981). Contrary to most local analysis schemes, the EC system calculates the analysis changes (increments) for a volume that is of a considerable size, approximately 1300 by 1300 km in the horizontal and a third of the atmosphere in the vertical. A volume of these dimensions generally contains at least a hundred data items which all simultaneously enter the OI equations. The main meteorological advantage of large analysis volumes in a multivariate OI scheme is the explicit mass and wind balance that can be imposed on the increments for relatively large scales.

For these idealised experiments we specify the field to be analysed, or strictly its departure from a guess field, by the following function

$$f^{obs}(r) = \begin{cases} \frac{1}{2}[1 + \cos(2\pi r/D)] & r \leq D/2 \\ 0 & r > D/2 \end{cases} \qquad (1)$$

in which r is the distance from the centre of the observation area and D is the diameter of the feature to be analysed. The "observations" are given on a regular grid (See Fig. 1) with values defined by (1).

The discussion will be restricted to the effect of the OI "operator" on the amplitude. The problems of aliasing in the analysis are deferred until Section 4. The amplitude response is measured by the ratio of the analysis increment to the observed departure at r=0. This ratio will be given as a function of two non-dimensional numbers, the normalised expected observation error

$$\varepsilon^o = \frac{E^{obs}}{E^{pred}} \qquad (2)$$

and a normalised length L = D/b. E^{obs} and E^{pred} are the observation and prediction errors; b is the scale length of the Gaussian horizontal forecast error correlation function

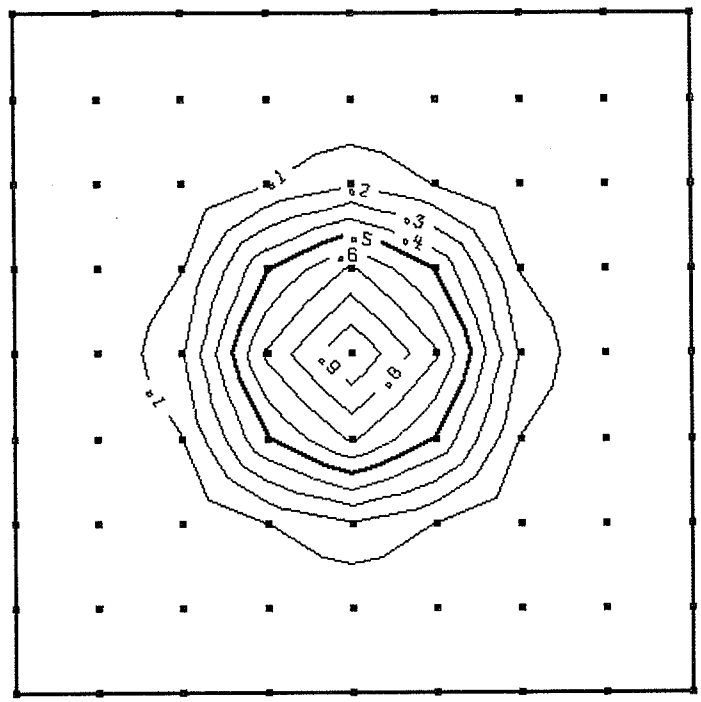

Fig. 1 The observation distribution in the idealised analysis experiments and an example of the "observed" field.

$$\Pi(r) = e^{-\frac{1}{2}(\frac{r}{b})^2} \qquad (3)$$

which is used for these calculations. In the EC analysis, b is specified as 600 km in the Northern Hemisphere.

As we use "observations" that represent the truth exactly, our results will give the upper limit of what we can expect under the most favourable conditions.

Firstly, the OI response will be established for a reference case. Secondly, the impact of increased data density and/or reduced matrix size on resolution will be discussed. Four different cases, characterised by the data density (0.25b or 0.125 b) and the matrix size (81 or 25 observations) are considered:-

a) observation density is 0.25b with 81 observations covering an area of 2b by 2b (See Fig. 1). This case is taken as reference.

b) observation density 0.125b and 81 observations - area is b by b.

c) observation density 0.25b but with only a 5 by 5 observation array around the mid point - the data area is then b by b.

d) observation density 0.125b and 25 observations - area is 0.5b by 0.5b.

Case a represents the situation in data dense areas. A 0.25b observation density corresponds in the EC system to a 150 km observation spacing. The data area is equivalent to a 1200 km square. In Fig. 2 (and in all other similar diagrams) the abscissa is the non-dimensional size of the feature, L=D/b, and the ordinate is the normalised observation error, ε^o . A typical value of the normalised observation error of a surface pressure measurement in the EC scheme is 0.4. For this value of the expected observation error

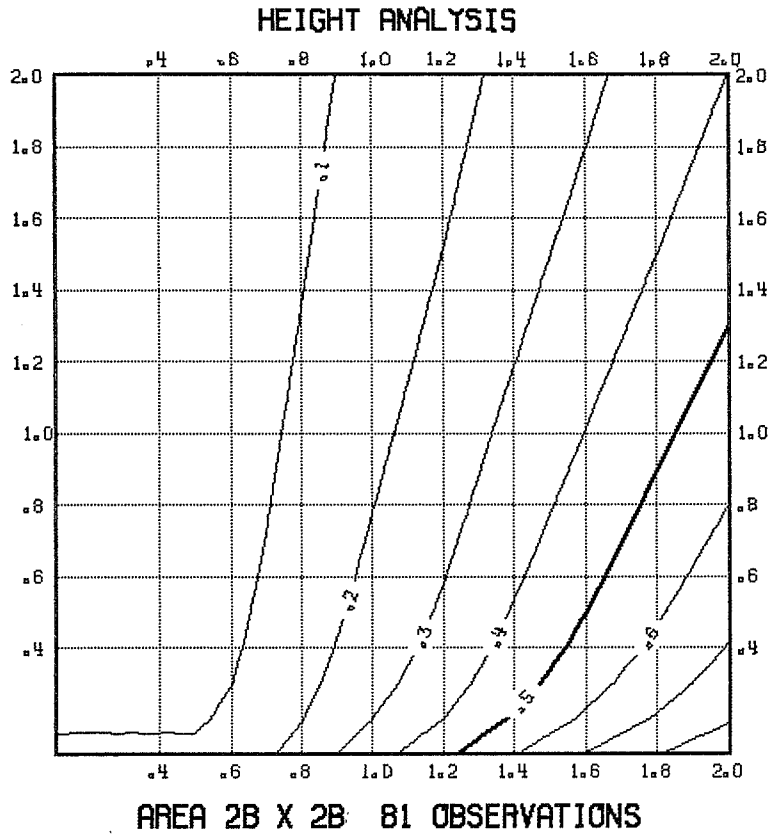

Fig. 2 Amplitude response of univariate OI analysis of height as function of scale, D/b (abscissa), and normalised observation error (ordinate). The observation density is 0.25 b and a regular quadratic array of 81 observations is used. The forecast error correlation model is Gaussian.

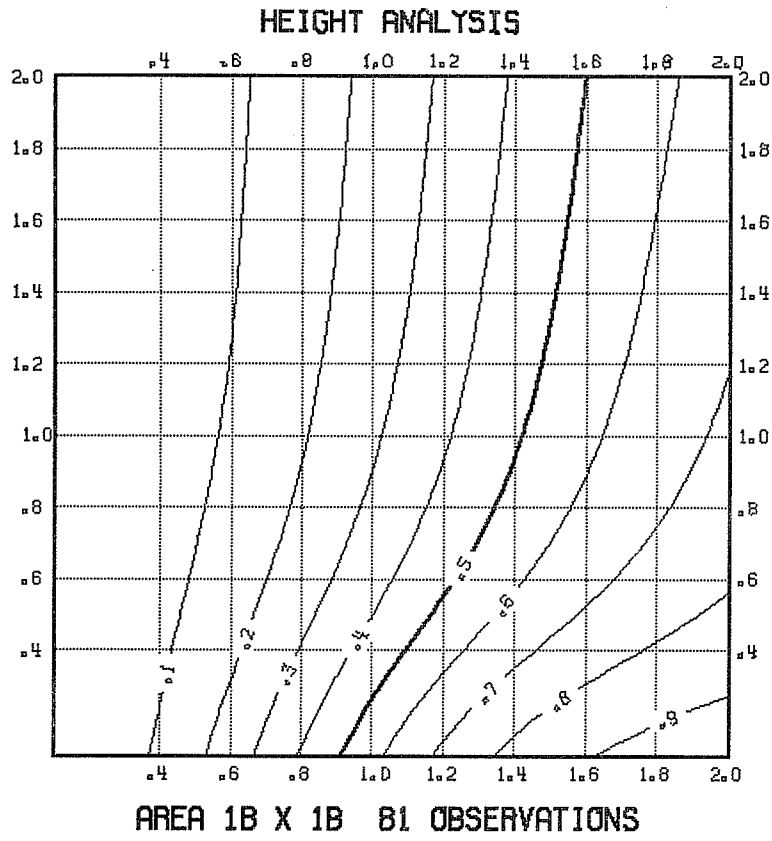

Fig. 3 Same as Fig. 2, except that the observation density is 0.125 b and the data area is b by b.

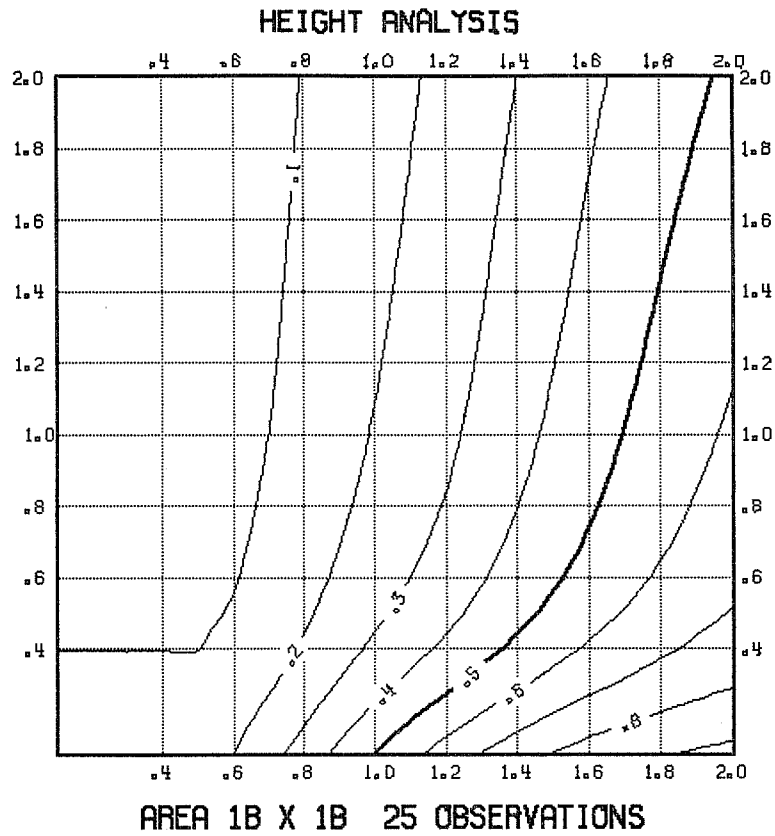

Fig. 4 Same as Fig. 2, except that only a 5 by 5 data array is used covering an area of b by b.

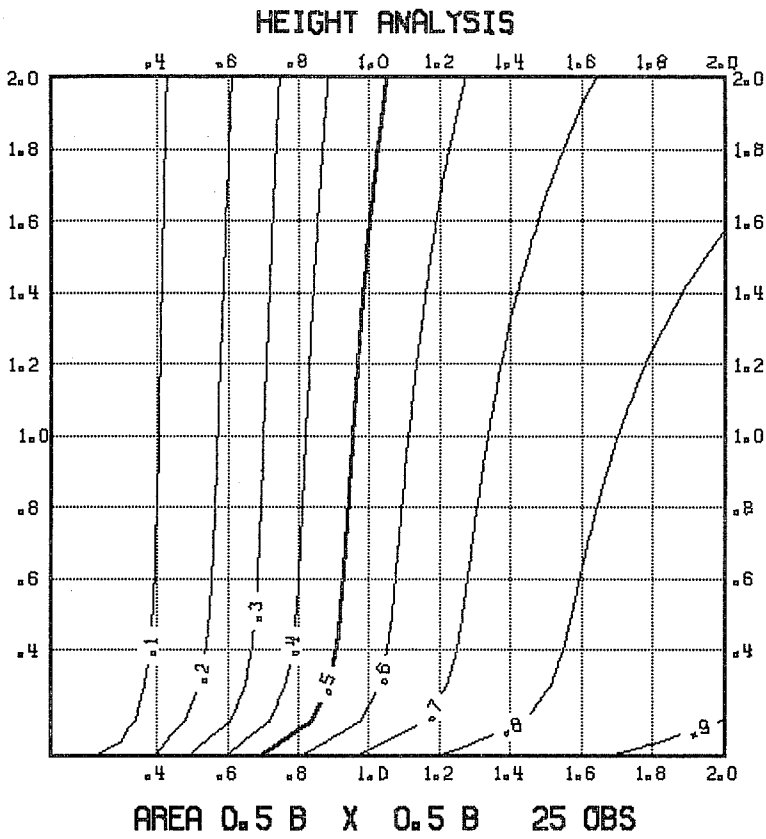

Fig. 5 Same as Fig. 2, except that only 25 observations are used with a data density of 0.125 b covering an area of 0.5 by 0.5 b.

even relatively large systems are damped. Of the original amplitude, 0.70 is retained for a disturbance with a diameter of 2b (1200 km) and only 0.25 when its diameter is b. Lower estimated observation errors naturally produce a better response to the observed values and their inaccuracies. The sensitivity to the assigned observation error is in general weak. A doubling of the error, from 0.4 to 0.8, reduces the response for a scale of 2b from 70% to 60%. For scales smaller than 2b the reduction of the amplitude decreases in absolute terms.

Next, the data density is doubled to 0.125b (75 km in the EC system), but keeping the matrix size the same (this is case b). The observation area is then reduced to b by b. Fig. 3 shows that systems of a diameter of 2b are well analysed (0.85) and about 43% of the amplitude is returned at b. The gain from the higher data density is about 0.15 units. An increase of the observation error from 0.4 to 0.8 produces a loss of approximately 0.1 units for scales between b and 2 b.

In case c, we investigate the effect of the matrix size on the analysis. In Fig. 4 only 25 observations with a spacing of 0.25b contribute to the analysis at the centre point. This gives a slight improvement over the case with 81 observations (Fig. 2). The analysed amplitudes are 0.75 for 2b and 0.32 for b, a gain of 0.05 and 0.07, respectively. As we use perfect data we avoid the problem of drawing to bad observations. Obviously, the damping of noise weakens as the matrix size decreases. Consequently, we should not try to extrapolate the improvement in analysis resolution obtained from reducing the matrix size from 81 to 25 data when perfect data is used.

In the final case (case d), we study the impact of increased data density with only 25 observations (Fig. 5). The responses are now 0.87 (2b) and 0.57 (b), an improvement from the reference case of 0.17 and 0.25 units, respectively. For observation errors larger than 0.5 the analysis becomes very insensitive to the assumed value of the error. Compared to the large area high density case (Fig. 3), the improvement depends strongly on scale - 0.02 at 2b and 0.15 at b. The results of the four cases are summarised in Table 1.

Table 1. The horizontal resolution of OI using a Gaussian structure function and a normalised observation error of 0.4 for two scales L = 1 and L = 2. The data density and number of observations is given in the left hand column.

Data network/ selection		L, Normalised scale of disturbance	
		1	2
	1) Δx = 0.25b 81 obs	0.25	0.70
	2) Δx = 0.125b 81 obs	0.43	0.85
	3) Δx = 0.25b 25 obs	0.32	0.75
	4) Δx = 0.125b 25 obs	0.57	0.87

Now let us assume that in a given synoptic situation we know that a smaller b would be more appropriate than the standard b. How much could then be gained in resolution by modifying b before the analysis. Apart from the reduced value of the scale parameter, all other aspects of the analysis including the data selection are identical. The effect on the resolution can be derived

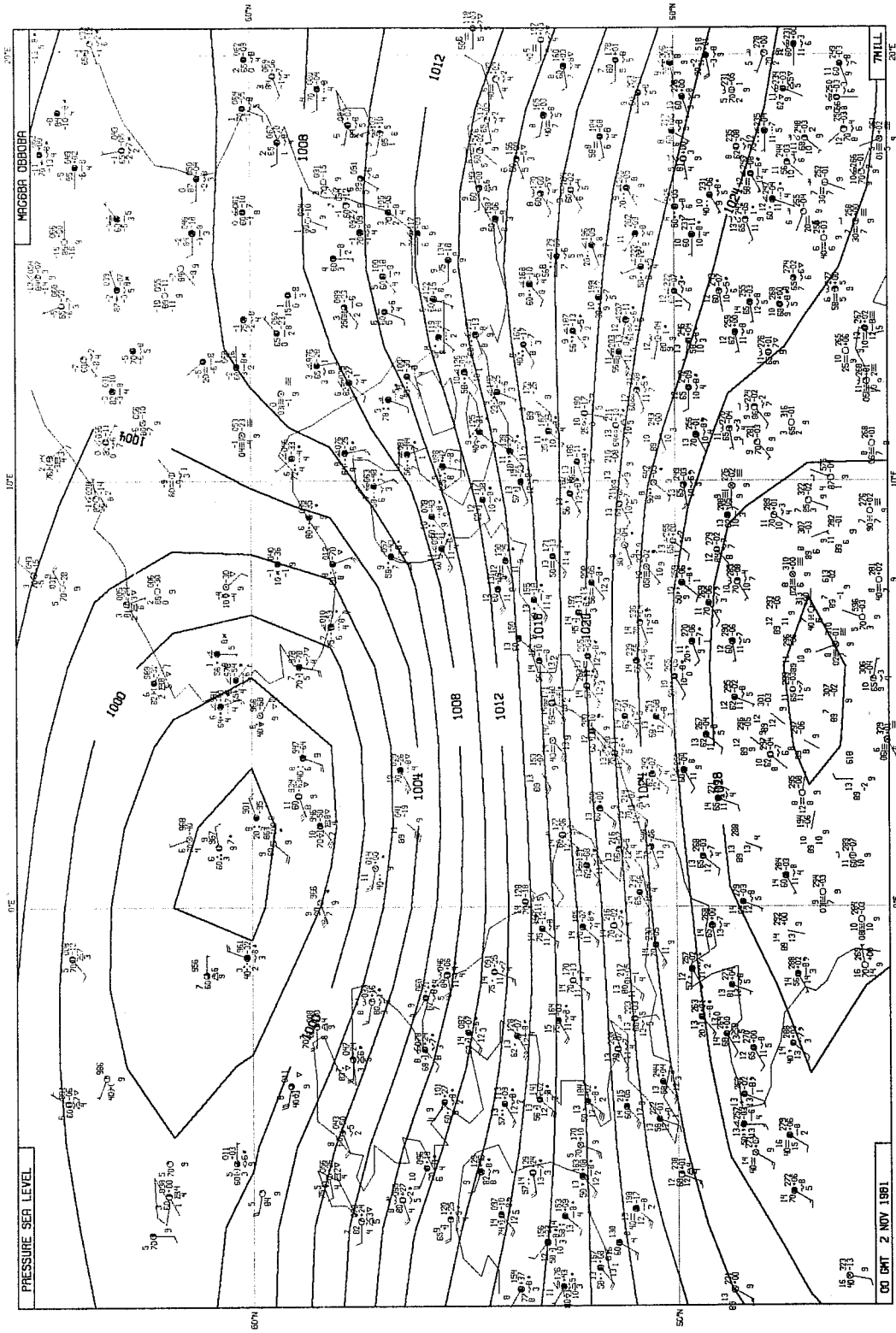

Fig. 6 Univariate height analysis using a Gaussian correlation function with b = 600 km.

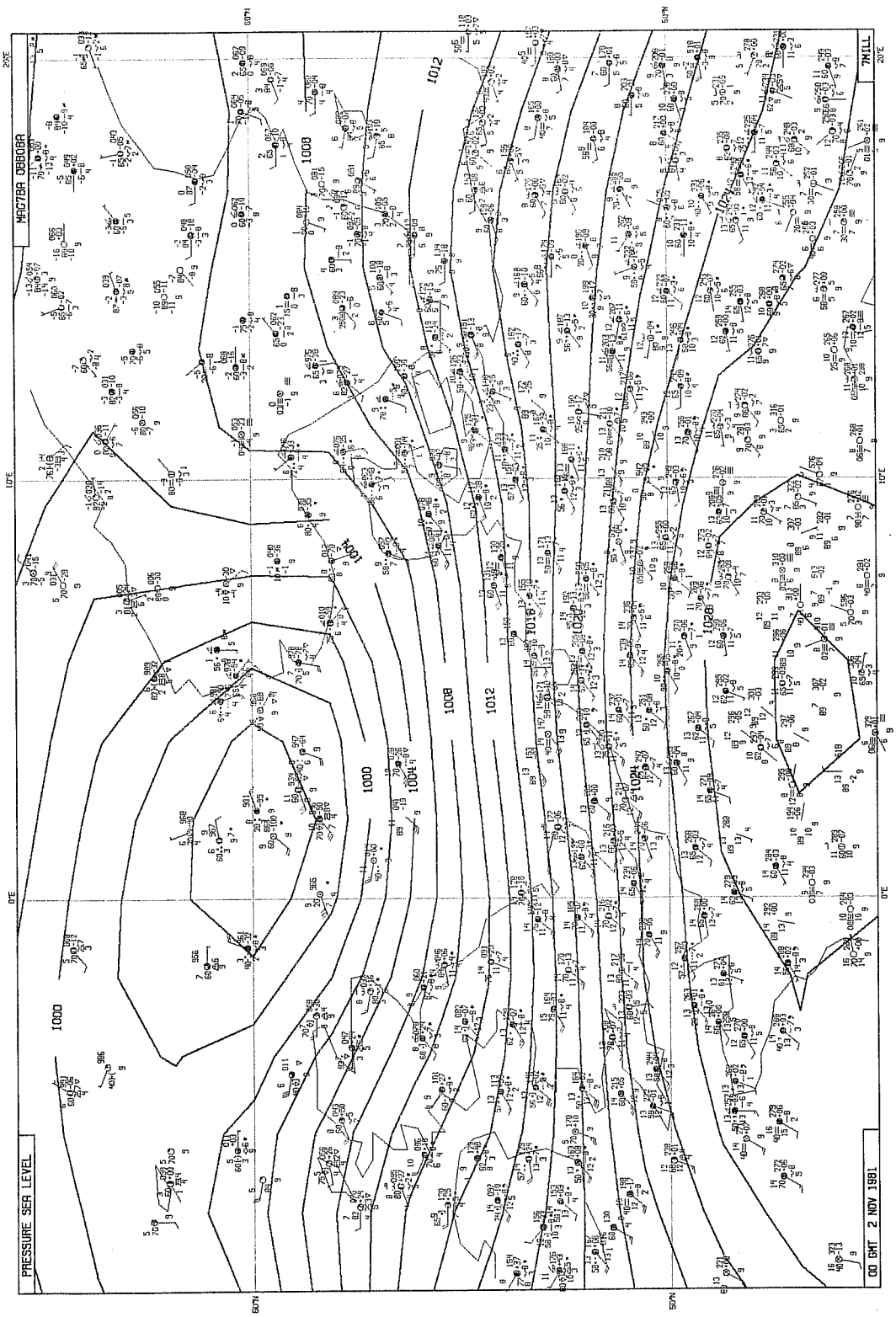

Fig. 7 Same as 6, but b = 300 km.

from the results presented above. We can compare the two cases with 81 observations (Figs. 3 and 2) as follows. In the standard b situation we assume a data density of 0.125 b. In the analysis with reduced scale parameter we assign b' = 0.5b and thus have a data density of 0.25 b'. Then one length unit in Fig. 3 corresponds to two units in Fig. 2. For a system that has a diameter of b = 2b', the response improves from 43% to 70%.

To test this conjecture in a real situation, we ran univariate three-dimensional height analyses for a case (2.11.81 00 GMT) with a developing depression over the North Sea. Two values of the horizontal correlation scale parameter were considered, b = 600 km (Fig. 6) and b = 300 km (Fig. 7). In both runs the surface pressure report of 986.3 mb from the platform at 59.5°N and 1.5°E was rejected. The deepest accepted pressure, 990.1 mb (59.9°N and 2.1°E), is approximately 10 mb from the first-guess. With b = 600 km, 45% of the difference is analysed (Fig. 6) and for b = 300 km this increases to 55% (Fig. 7). This reduction of analysis error is less than expected from the above theoretical calculations because the present structure of the EC analysis scheme is not very favourable for high resolution analysis. The final analysis increment at a gridpoint is formed as a weighted mean of several analyses calculated from neighbouring partly overlapping data sets. In situations of high data density, the data selection is not extensive enough to cover the whole analysis area and significant differences between the analysis increments for the same point may arise.

An overall improvement in the fit of the analysis to the data follows from the reduced value of b. This agrees with Seaman's (1977) calculations, in which he found that sub-optimal values of b produced lower analysis errors than the optimal b for the geopotential. However, he also showed that an underestimate of b degraded the analysis of the gradient and Laplacian of the field. Consequently, in a multivariate environment improved horizontal

resolution can not be achieved by reducing the value of b without seriously affecting the wind analysis.

2.2 Analysis of wind

Similar amplitude response calculations have been carried out for the wind analysis using wind data only. The wind "observations" are derived geostrophically from (1). The measure of response is the vorticity of the analysed wind as compared to the initial vorticity (the vorticity is estimated by a second order centered finite difference approximation). Fig. 8 presents the response of the wind analysis as a function of scale and observation error. A typical normalised observation error for a radiosonde wind measurement is approximately 1.0. For systems with a diameter of 2.0 b, slightly more than half is kept, whereas for scales of the order of b, less than 10% is returned.

3. COMPARISON OF CORRELATION FUNCTIONS

3.1 Gaussian correlation model

The weaknesses of the Gaussian structure function have been discussed by Julian and Thiebaux (1975). The energy spectrum of the Gaussian correlation function is an exponential of the squared wavenumber with only one scaling parameter, b. The decay rate of the energy spectrum of the exponential correlation function is faster at high wavenumbers than implied by the observed spectrum. This results in a poor fit to empirical forecast error correlations and a strong sensitivity to the range of distance separation of the correlation data. Figs. 9a and 9b clearly demonstrate the weaknesses of the exponential to fit observed-minus-forecast correlations. The empirical correlations are based on a 12 day sample of departures of North American radiosonde observations from the corresponding first-guess (6 hour forecast) values. Correlations of the departures between all station pairs have been calculated. The correlations are grouped according to separation distance and averaged in 25 or 50 km intervals. Through these group correlations an exponential with two free parameters is fitted

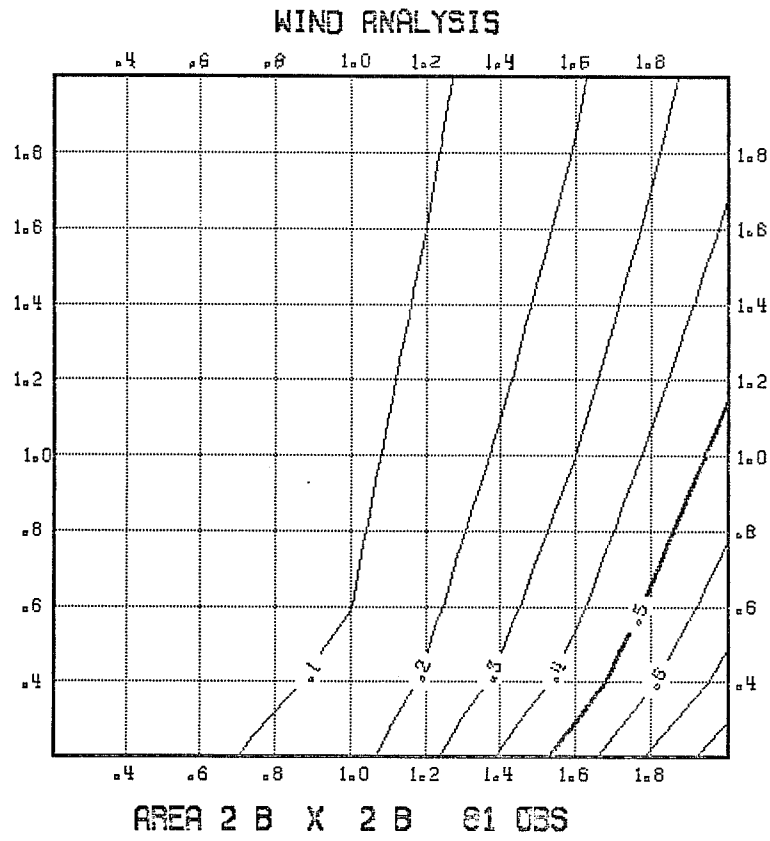

Fig. 8 Amplitude response for vorticity as function of scale, D/b (abscissa), and normalised observation error (ordinate). The observations are given on a regular 9 by 9 array (see Fig. 1) with a spacing of 0.25 b.

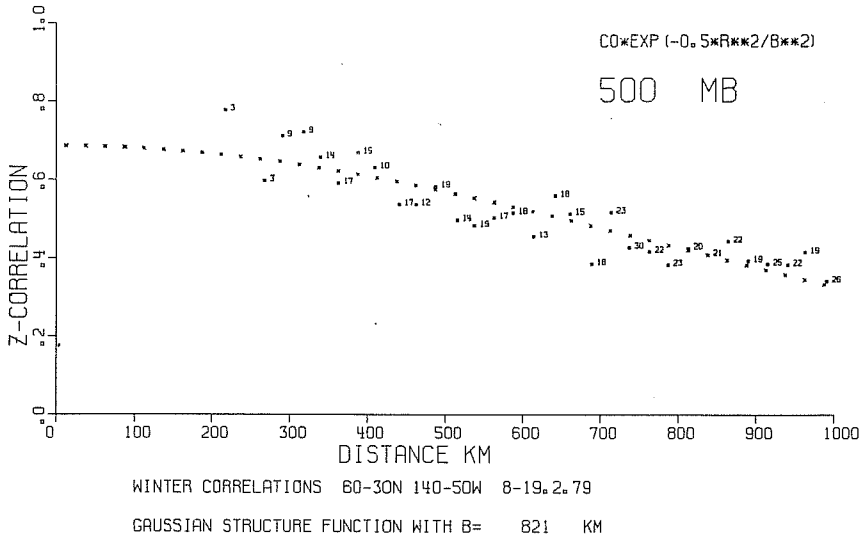

Fig. 9a Empirical 500 mb height forecast error correlations averaged over 25 km intervals. An exponential with two free parameters has been fitted to the interval average correlations. All station pairs up to a distance of 1000 km have been used.

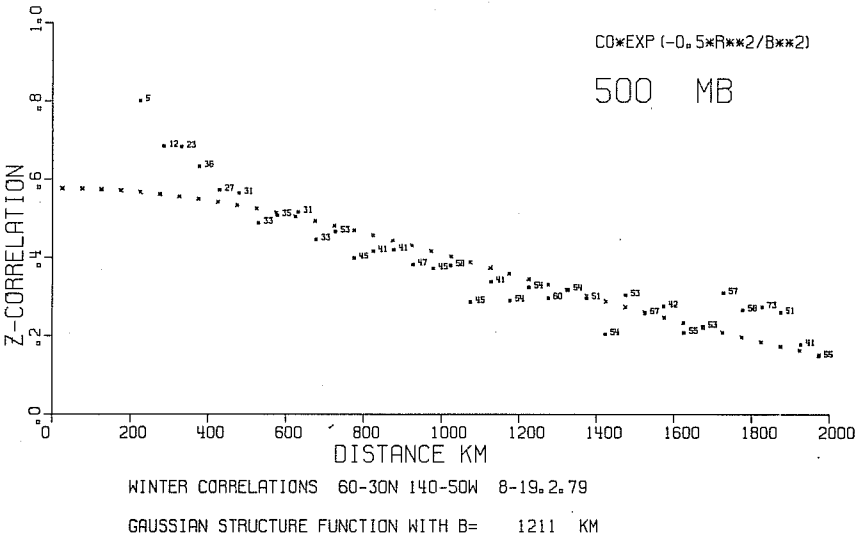

Fig. 9b Same as 9a, but for a maximum distance of 2000 km and 50 km intervals.

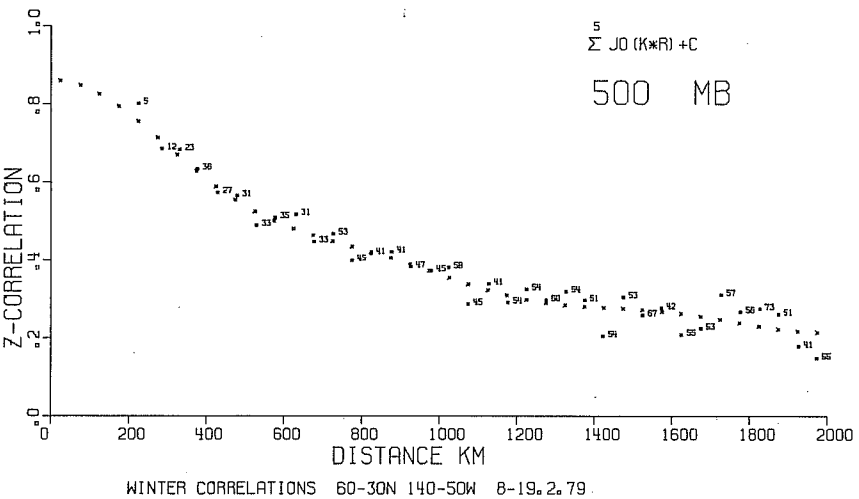

Fig. 9c Same as 9b, but for the Bessel function model.

$$\Pi^*(r) = ce^{-\frac{1}{2}(\frac{r}{b})^2} \qquad (4)$$

in which c is the zero intercept correlation and b is the correlation scale length. The parameters were determined by a least squares best fit algorithm for two observation separation ranges, 200 to 1000 km (25 km intervals) and 200 to 2000 km (50 km intervals). The values of b show a strong dependence on the separation range. The sharpness of the empirical correlations at small separations (up to 500 km) can not be resolved by the exponential.

3.2 Bessel function correlation model

Many reasonable candidates for functional representation of the empirical correlations exist (Julian and Thiebaux, 1975). The Fourier transform pair of a two-dimensional isotropic correlation function involves Bessel functions of zero order and of the first kind, J_o. Consequently, a correlation representaion based on a series of Bessel functions is particularly suitable (Rutherford, 1972):

$$\Xi(r) = \sum_{i=1}^{N} A_i J_o(k_i \frac{r}{R}) + A_o \qquad (5)$$

in which k_i is the i'th root of J_o. The coefficients A_i (i=0,...N) are determined by a least squares fit to empirical correlations in the domain (0,R). With several free parameters, a close fit to the data is expected. The series is truncated at the first negative coefficient which implies negative power for the corresponding two-dimensional wave (Gandin, 1963 and Rutherford, 1972). To fit (5) to correlation data is equivalent to calculating the two-dimensional Fourier transform of the correlations. Correlation representation (5) has the properties required for the existence of geostrophic wind correlations (Julian and Thiebaux, 1975).

Function (5) has been fitted to the same data set as the Gaussian with R=2000 km and N=5. A visual comparison of Figs. 9b and 9c demonstrates the

superiority of the Bessel functions over the Gaussian in reproducing the empirical correlations. Obviously, the spectral properties of the two correlation representations are quite different.

3.3 Amplitude response to Bessel function model

The amplitude response analysis has been repeated for the Bessel functions using the coefficients returned by the least squares algorithm applied to the 500 mb height correlation data. Again, the results are displayed as a function of observation error (ordinate) and normalised length scale, $L = D/600$ km, (abscissa). Consequently, the figures of Section 2 are comparable if $b = 600$ km is assumed for the Gaussian. Fig. 10 shows the case of data density 0.25b and 81 observations. A considerable improvement in a univariate height analysis is produced by using the Bessel function model (compare Figs. 10 and 2). However, an overshoot is evident for scales larger than 1.8 b implying a possible deteoriation compared with the Gaussian for large scale analysis.

The damping by the OI "operator" is very weak at scales of the order of 2b and consequently no improvement can be expected on these scales from increased data density or reduced matrix size. For systems with a diameter of b, a considerable benefit in resolution comes from increased data density (compare Figs. 11 and 10).

The impact on the horizontal resolution of changes in the matrix dimensions is minor in both the 0.25b case (compare Figs. 12 and 10) and in the 0.125b case (compare Figs. 13 and 11). This result suggests that we can have a fairly large data domain without seriously affecting the resolution. Table 2 summarises the analysis responses for the Bessel functions.

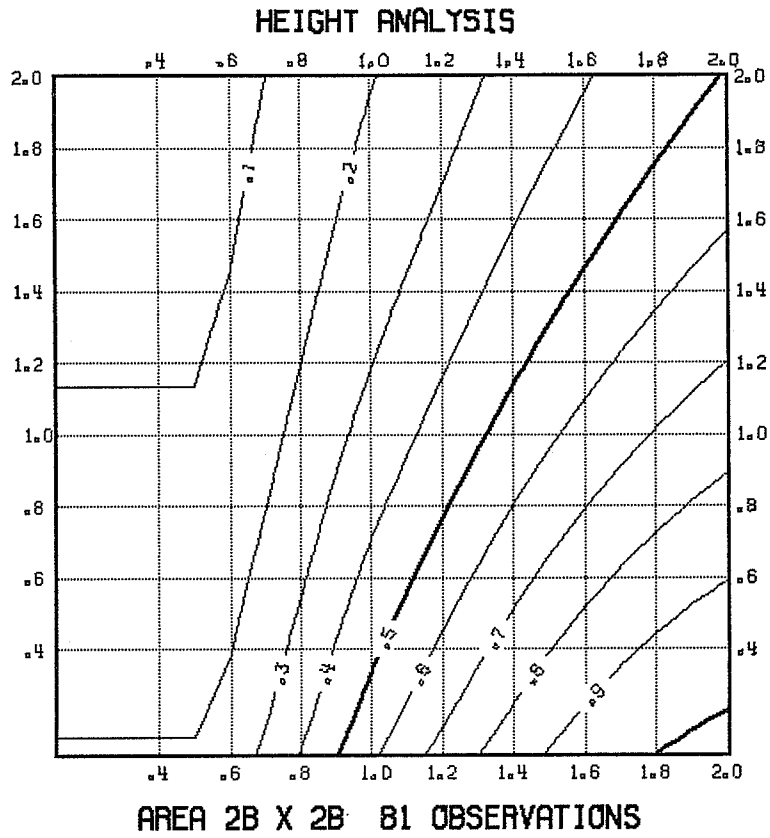

Fig. 10 Amplitude response for univariate height analysis as function of scale, D/600 km (abscissa), and normalised observation error (ordinate). The observation density is 0.25 b and 81 observations on regular grid have been used in the calculations. The forecast error model is based on a series of Bessel functions.

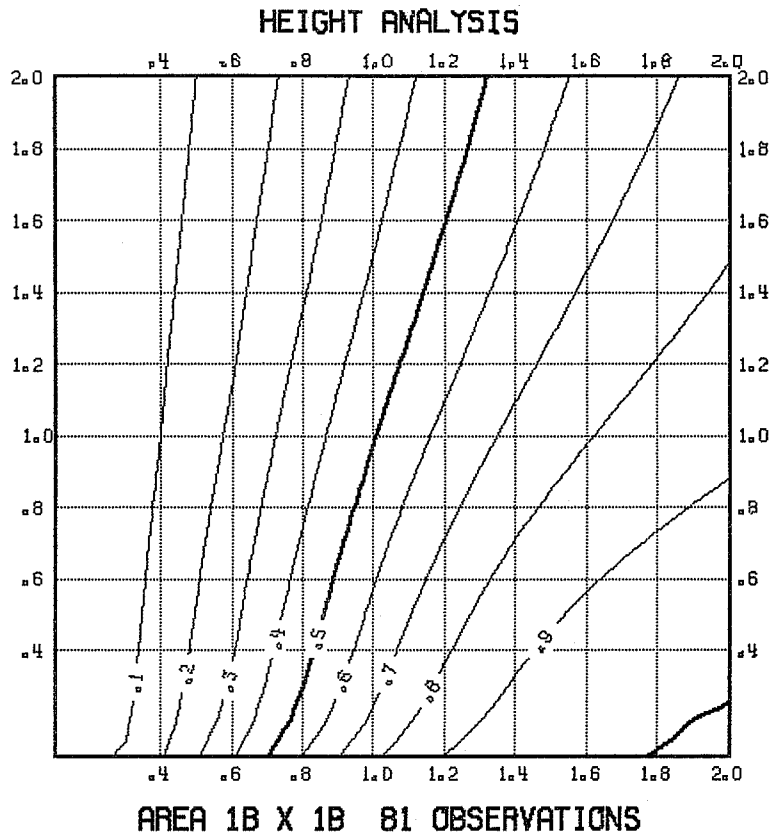

Fig. 11 Same as Fig. 10, except for data density of 0.125 b.

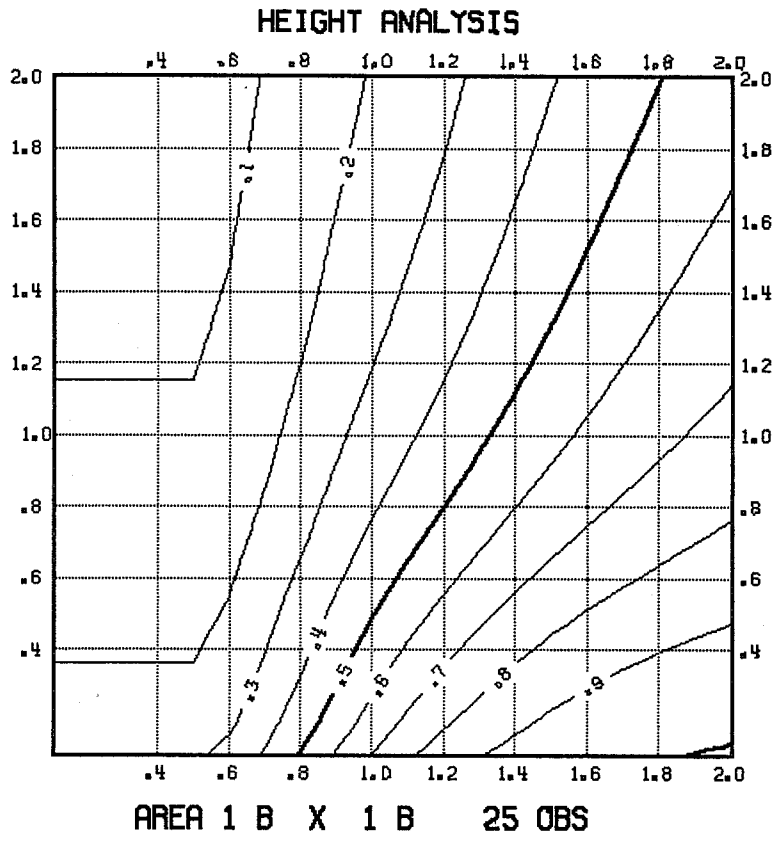

Fig. 12 Same as Fig. 10, except that only a 5 by 5 data array is used.

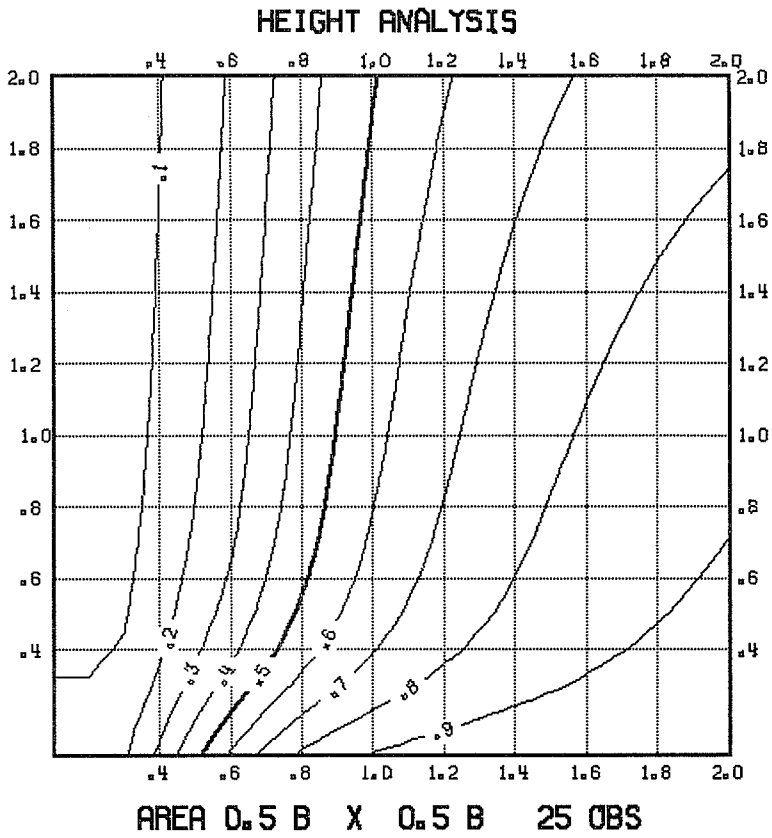

Fig. 13 Same as Fig. 10, except that only 25 observations with a data density of 0.125 b is used.

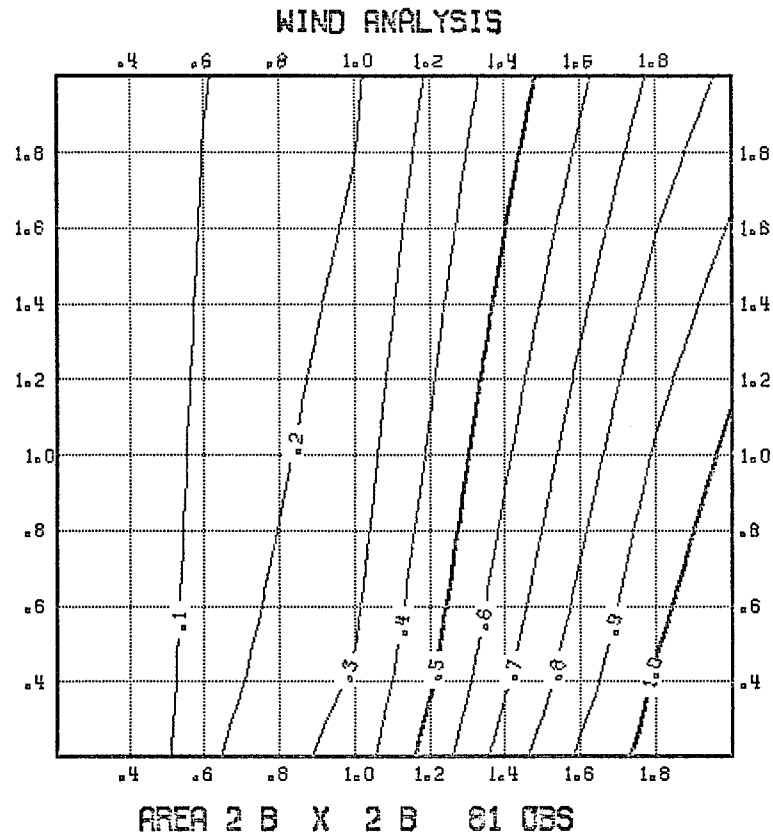

Fig. 14 Same as Fig. 8, but with the Bessel function model.

Table 2. As for Table 1 , with Bessel function model.

Data network/ selection		L, Normalised scale of disturbance 1	2
	1) Δx = 0.25b 81 obs	0.47	0.94
	2) Δx = 0.125b 81 obs	0.63	0.97
	3) Δx = 0.25b 25 obs	0.53	0.92
	4) Δx = 0.125b 25 obs	0.70	0.94

An overall gain of approximately 0.2 units can be obtained from the use of the Bessel function model instead of the Gaussian (see Tables 1 and 2). A more striking result is the weak dependence of the resolution on the matrix size for the Bessel functions. Consequently, this correlation model offers us improved horizontal resolution without relaxation of the mass and wind balance.

The resolution of the wind analysis improves by using Bessel functions, as can be seen by comparing Figs. 14 and 8. However, the Bessel function model may give a poorer analysis of the large scale wind analysis than the Gaussian model as is suggested by the amplification of the "observed" vorticity at scales of 2b (Fig. 14).

3.4 Univariate analysis with Bessel function model using real data

The results of the previous sections suggest that at least univariately, the Bessel functions should improve the small scale analysis. To test this hypothesis with real data, a univariate height analysis was run with the Bessel function model for the same case as described in Section 2. The

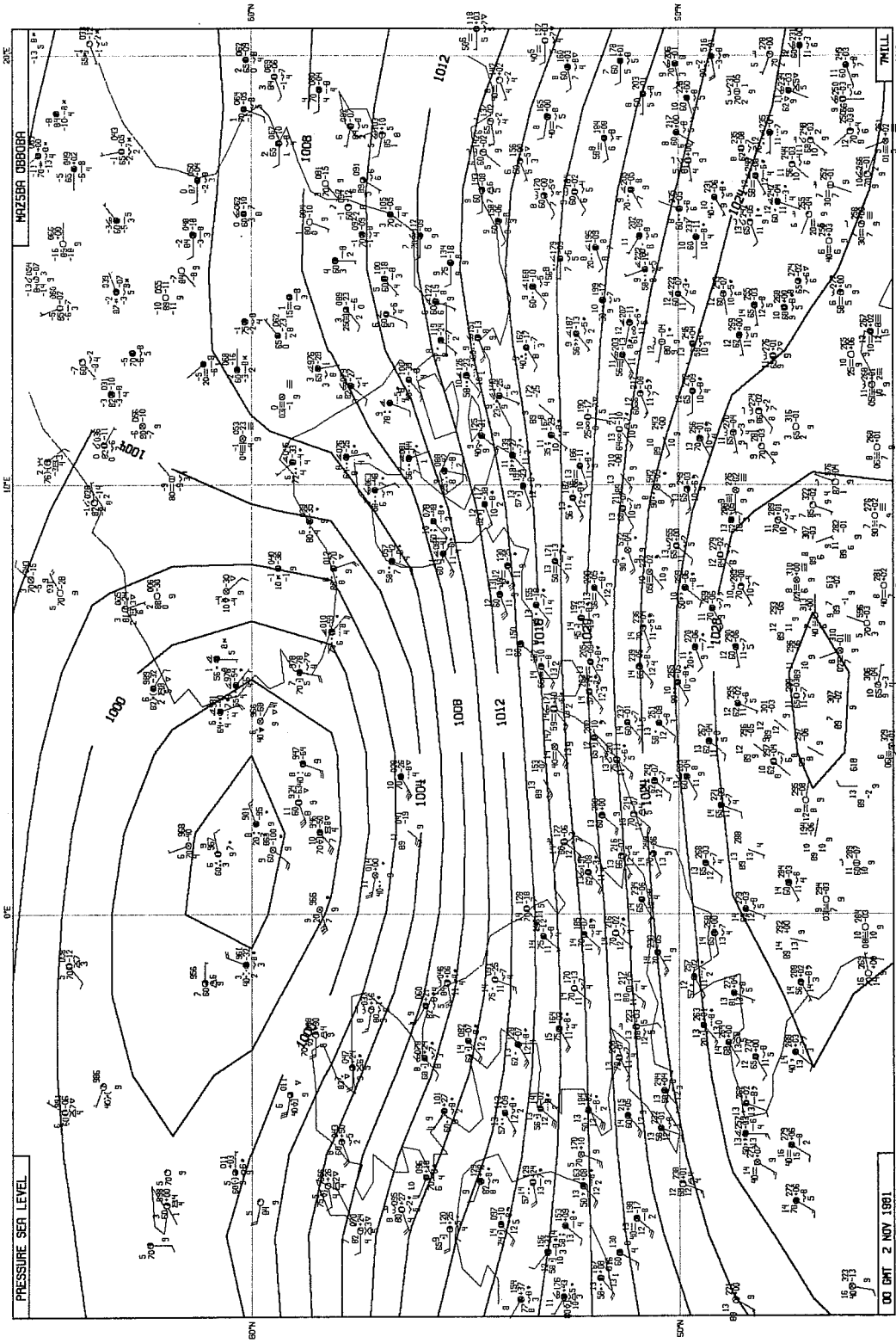

Fig. 15 Univariate height analysis using a Bessel function forecast error model.

improvement over the Gaussian with b = 600 km is very modest, from 45% to 50% of the observed departure, as can be seen by comparing Figs. 15 and 6. The failure to capture more of the depth of the depression can be explained by the structure of the EC scheme as was already discussed in detail in Section 2.1

4. EIGENVECTOR EXPANSION OF OI

Statistical interpolation can be thought of as a linear operator applied to data. A powerful method of studying the properties of OI is spectral decomposition of this linear operator. The method (see Section 6 by Hollingsworth in Lönnberg and Hollingsworth, 1983) is derived in Section 4.1. In 4.2 and 4.3 we apply the technique to univariate height and wind analyses and compare the properties of the Gaussian and Bessel function correlation models.

4.1 Method

The analysis for a point and variable, A, is expressed by

$$A = \underline{W}^T \underline{D} \tag{6}$$

in which the elements of $\underline{W}$ are the weights given to the corresponding observed data $\underline{D}$. If the same data set is used for the analysis at several points, we can combine the weight vectors into a matrix and express (6) compactly by

$$\underline{A} = \underline{\underline{W}}^T \underline{D} \tag{7}$$

If the analysis points coincide with the data points and represent the same variable, then the weights are given by

$$\underline{\underline{W}} = (\underline{\underline{P}} + \underline{\underline{O}})^{-1} \underline{\underline{P}} \tag{8}$$

in which $\underline{\underline{P}}$ is the prediction error covariance matrix for all possible combinations of observations. $\underline{\underline{O}}$ is the corresponding observation error covariance matrix.

$\underline{\underline{P}}$ (real and symmetric) can be expanded in terms of its eigenvectors and eigenvalues as follows

$$\underline{\underline{P}} = \underline{\underline{E}}\ \underline{\underline{\Lambda}}\ \underline{\underline{E}}^T \tag{9}$$

in which $\underline{\underline{E}}$ is a matrix of orthonormal eigenvectors and $\underline{\underline{\Lambda}}$ is a diagonal matrix of the corresponding eigenvalues.

The observation errors are assumed to be uncorrelated and constant. Consequently, $\underline{\underline{O}}$ can be written as

$$\underline{\underline{O}} = \sigma^2 I = \underline{\underline{E}}\ (\sigma^2 I)\ \underline{\underline{E}}^T \tag{10}$$

The observations $\underline{D}$ can be written as a linear combination of the eigenvectors $\underline{\underline{E}}$

$$\underline{D} = \underline{\underline{E}}\ \underline{\Gamma} \tag{11}$$

where $\underline{\Gamma}$ is the coefficient vector of the eigenvectors.

By inserting (9) and (10) into (8), the weights may expressed as follows

$$\underline{\underline{W}} = \underline{\underline{E}}\ (\underline{\underline{\Lambda}} + \sigma^2 I)^{-1}\ \underline{\underline{\Lambda}}\ \underline{\underline{E}}^T \tag{12}$$

The expression for the analysis is obtained by inserting (12) and (11) into (7) and using the orthogonality of $\underline{\underline{E}}$ ($\underline{\underline{E}}\underline{\underline{E}}^T = I$) to give

$$\underline{\underline{A}} = \underline{\underline{E}}\ (\underline{\underline{\Lambda}} + \sigma^2 I)^{-1} \underline{\underline{\Lambda}}\underline{\Gamma} \tag{13}$$

The analysed amplitude of mode i is then

$$\frac{\lambda_i}{\lambda_i + \sigma^2}\ \gamma_i^2 \tag{14}$$

Consequently, the damping of a particular observed mode is

$$1 - \frac{\lambda_i}{\lambda_i + \sigma^2} = \frac{\sigma^2}{\lambda_i + \sigma^2} \tag{15}$$

Positive definiteness of $\underline{\underline{P}}$ guarantees that all eigenvalues are positive. It is readily seen from (15) that when the eigenvalue is small compared to the observation error variance the mode is heavily damped. Similarly, modes with large eigenvalues remain almost intact.

The eigenvector analysis is applied in one dimension to univariate height and wind OI and the results are presented in the following sections.

4.2 Height analysis

The spectral technique developed in Section 4.1 is applied in one dimension to 9 evenly spaced observations and gridpoints. In the results that are presented in this section and the following one, we only show the four gravest modes as the power of the remaining modes is mostly negligible. Furthermore, this section provides some answers to questions raised in Section 2 related to aliasing in the analysis.

In Section 2 it was shown that the exponential correlation function excessively damped the smallest scale. This becomes more evident from Fig. 16 in which the four gravest eigenmodes are displayed. The corresponding eigenvalues are 6.62, 2.02, 0.33 and 0.03. For a typical normalised observation error of 0.4, the third mode is already heavily damped (67% of the amplitude remains). Conseqently, only the mean and a linear variation through the domain can be analysed satisfactorily. However, selective damping of different modes causes aliasing that may be harmful for the large scale analysis. As an example we take the analysis of an observed constant field. Expansion of this in terms of the eigenvectors produces symmetric modes dominated by modes 1 and 3. The damping by the OI operator of mode 1 is very weak, but not insignificant for the other modes. As a result the structure of the analysis will resemble mode 1 that has a local extreme at the centre of the analysis area.

The improvement in resolution by using Bessel functions is also seen in Fig. 17. The structure of the first four modes is similar to those of the exponential correlation, but damping on modes 3 and 4 is significantly weaker.

4.3 Wind analysis

The geostrophically derived longitudinal wind correlation is identical to the height correlation for the exponential forecast error model. We can then use the results of Section 4.2, and in particular Fig. 16, to deduce the analysis response to wind observations. For a typical normalised wind observation

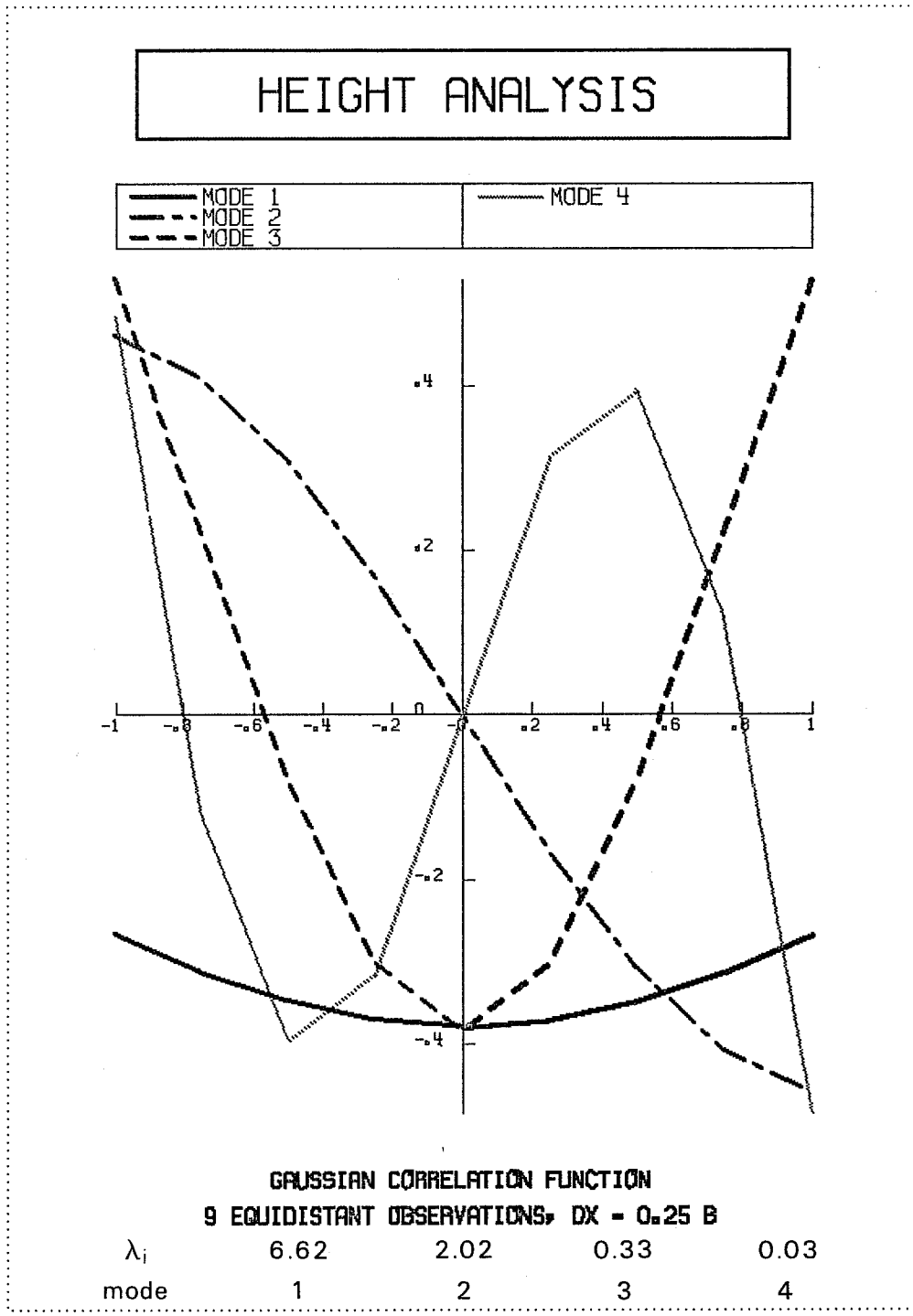

Fig. 16 The first four eigenvectors and the corresponding eigenvalues for a height analysis using the Gaussian structure function.

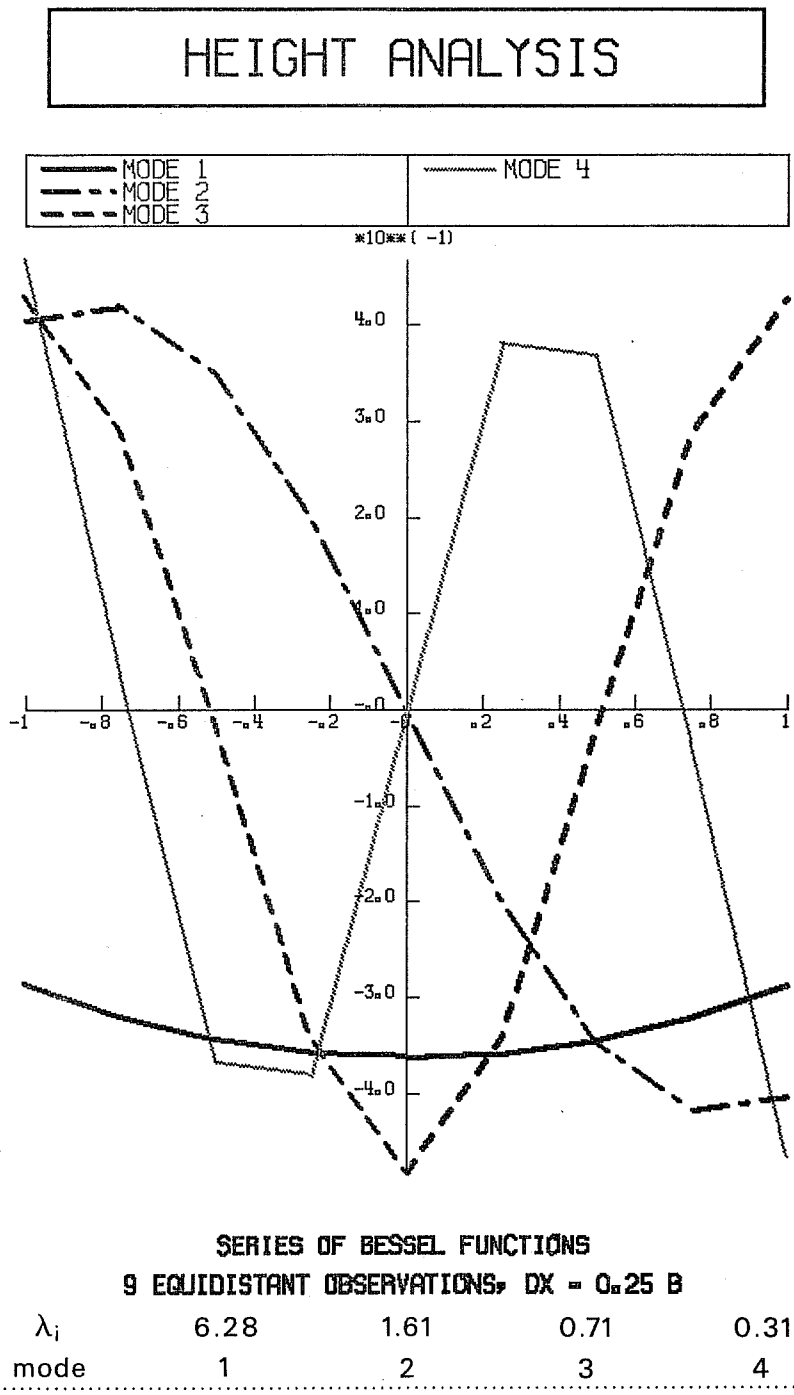

Fig. 17 Same as 16, but with the Bessel function model.

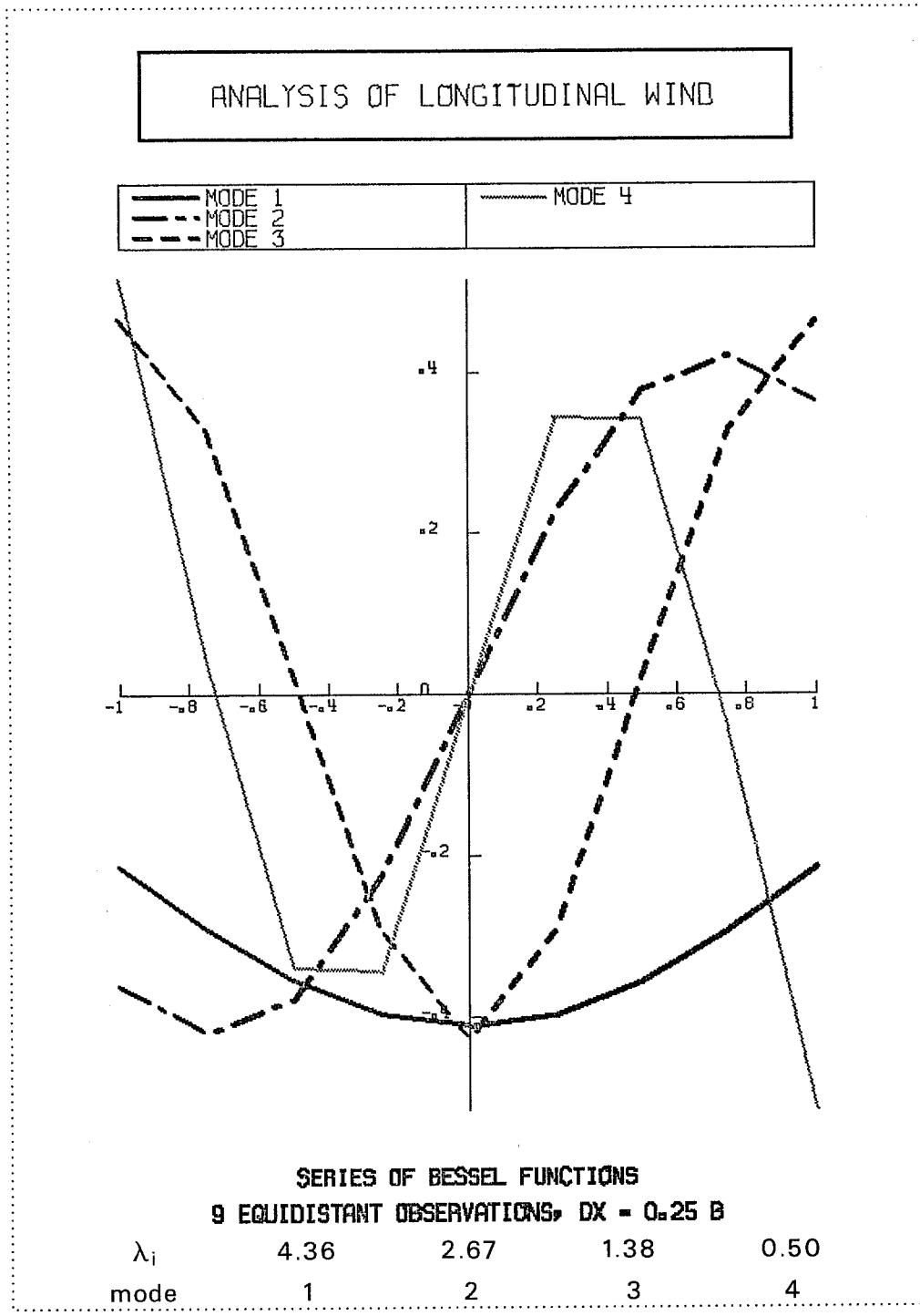

Fig. 18 The first four eigenvectors and corresponding eigenvalues for an analysis of longitudinal wind using a Bessel function correlation model.

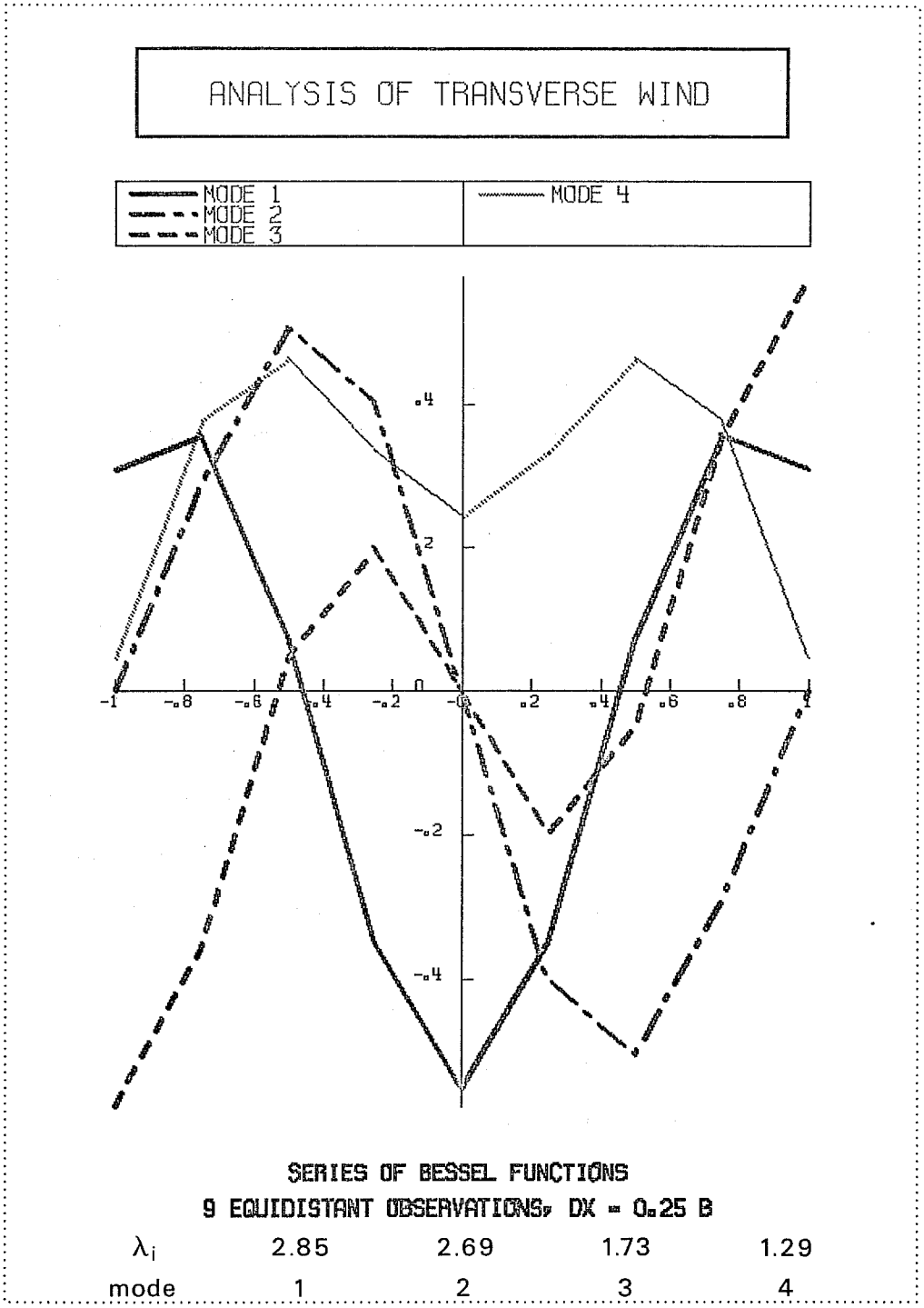

Fig. 19 Same as Fig. 18, but for the transverse wind.

error of 1, only modes 1 and 2 are well preserved; of mode 3, which has a half-wavelength of 2 b, only 25% remains.

Fig. 18 presents the eigenvectors and eigenvalues for the longitudinal wind using the Bessel functions. The sharpness of the correlation (not shown), derived geostrophically from height, for small separation distances produces a narrower distribution of the eigenvalues and in particular gives larger eigenvalues for modes 3 and 4 than the Gaussian. The Bessel function model thus responds to a wider range of input modes and has a weaker noise damping than the Gaussian model.

In the direction perpendicular to the flow, the wind correlation decreases rapidly and becomes negative. The distribution of the eigenvalues is very sensitive to the observation spacing as is discussed in detail by Hollingsworth in Lönnberg and Hollingsworth (1983). The results presented here are for only one observation spacing (0.25 b). For this data density the Bessel function model produces eigenvalues that cluster around unity (Fig. 19). Clearly, almost any wind distribution can be analysed with the Bessel functions and the noise control of the transverse wind is very weak in the analysis. The Gaussian model produces a wider spread of the eigenvalues (not shown) than the Bessel functions and is more effective in removing noise in the data.

5. CONCLUSIONS

The horizontal resolution of the current ECMWF analysis has been established. It is shown that the Gaussian correlation model severely limits the resolution of the OI scheme. Increased data density or reduced matrix size result in improved resolution at the expense of the mass and wind balance. Futhermore, the exponential correlation function seriously distorts the observed error spectrum of the six hour forecast.

An alternative correlation model based on a series of orthogonal Bessel functions has been studied. It was found that it reproduces the empirical correlations with satisfactory accuracy. As a consequence of faithful representation of the small scale structure of the forecast errors, a considerable theoretical improvement in horizontal resolution is achieved over the Gaussian. The structure of the EC system inhibits full exploitation of these properties and the benefit was modest in a case study with real data. The geostrophically derived transverse wind correlations created a noisy wind analysis due to their sharpness.

Aliasing of large scale modes was explained by means of spectral decomposition of the OI operator. The problem is enhanced by sharper structure functions.

The small amplitude of the changes produced by the initialisation in the EC system is a result of the geostrophic constraint imposed by the multivariate OI scheme on the mass and wind increments for large analysis volumes. The horizontal resolution of statistical interpolation with a Gaussian forecast error model depends strongly on the matrix size. This dependence is significantly weakened if the forecast errors are modelled by a series of Bessel functions. It was also shown that fine scale information in high resolution data is less strongly damped by the Bessel function model than by the Gaussian.

REFERENCES

Andersen, J.H. 1983 Experiments in boundary layer analysis with the ECMWF system. ECMWF Workshop on Current Problems in Data Assimilation.

Cats, G.J. and Wergen, W. 1983 Analysis of large scale normal modes by the ECMWF analysis scheme. ECMWF Workshop on Current Problems in Data Assimilation.

Gandin, L.S. 1963 Objective analysis of meteorological fields. Translated from Russian by Israeli Program for Scientific Translations, 1965, 242 pp.

Julian, P.R. and Thiebaux, H.J. 1975 On some properties of correlation functions used in optimum interpolation schemes. Mon.Wea.Rev., 103, 605-616.

Lorenc, A.C. 1981 A global three-dimensional multivariate statistical interpolation scheme. Mon.Wea.Rev., 109, 701-721.

Lönnberg, P. and Hollingsworth, A. 1983 ECMWF Lecture Note on Meteorological data analysis

Rutherford, I.D. 1972 Data assimilation by statistical interpolation of forecast error fields. J.Atmos.Sci., 29, 809-815.

Seaman, R.S. 1977 Absolute and differential accuracy of analyses achievable with specified observational network characteristics. Mon.Wea.Rev., 105, 1211-1222.